Chapter 6

In situ synthesis of green bionanocomposites based on aqueous citric acid cured epoxidized soybean oil-carboxylic acid functionalized MWCNTs

GRAPHICAL ABSTRACT

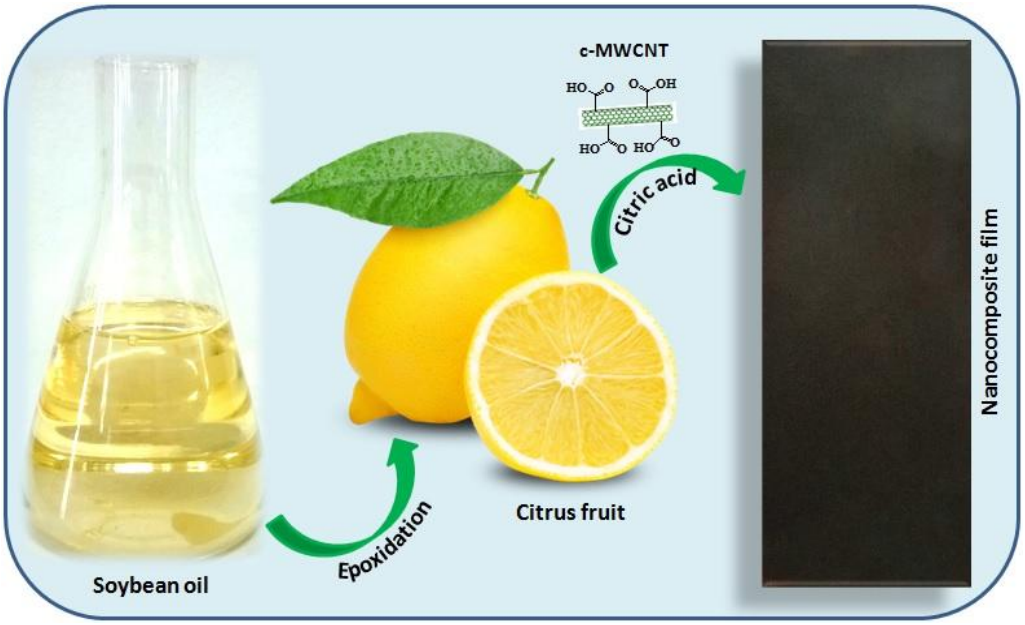

6.1 Introduction

Environmental concerns and the high rate of depletion of petroleum resources have triggered a great interest in the development of materials based on renewable resources. Among the different kinds of renewable raw materials, vegetable oils attracted much more attention due to their economic, environmental, and social advantages.[1-4] Moreover, assorted chemical modifications can be performed on vegetable oils, yielding functionalized vegetable oils (FVOs) that can be used to obtain diverse products.[5] Sun and Wool reported a detailed depiction of possible chemical modifications that can be performed on vegetable oils to obtain diverse FVOs, many of which are very useful in industrial applications.[6] Epoxidation of vegetable oils is one of the most important chemical modifications which can be achieved by the acid-catalyzed,[7] or the enzymatic processes.[8,9] The basic difference in the chemical structures of triglyceride obtained from various oilseeds is the fatty acid composition and the amount of double bonds. Soybean oil is an important vegetable oil offering a wide range of advantages. Soybean oil contains a large number of double bonds (oleic acid ~23%, linoleic acid ~53%, and alpha-linolenic acid ~9% with 1, 2, and 3 number of unsaturations respectively), giving an average of about 4.6 double bonds per triglyceride, and accordingly produces an epoxidised oil with high functionality.[10]

Soybean oil provides advantages as potential renewable raw material for industrial applications due to its worldwide availability in large scale. Presently, the US is the top producer of soybean oil in the world.[11] Now a days, epoxidized soybean oil (ESO), which

A part of this chapter is published

P. Gogoi, H. Horo, M. Khannam, S.K. Dolui, *Industrial Crops and Products* 2015, 76, 346–354.

is obtained easily from soybean oil is produced industrially at large scale and commercially available is bring forward to synthesize polymers by using its epoxy groups. Polymer networks can be obtained by ring opening polymerization of ESO with polyamine, polyacid or anhydride. Wang et al. reported the synthesis of a series of soybean-oil-based elastomers, poly(epoxidized soybean oil-co-decamethylene diamine) (PESD) by ring-opening polymerization of ESO with decamethylene diamine (DDA) in different molar ratios. The elastomers exhibited a wide range of applications with favorable processability and tunable properties.[12] Recently, Altuna et al. has reported the preparation of a class of "green" polymeric materials based on the cross-linking of epoxidised soybean oil by an aqueous citric acid solution. The self-healing ability of the polymer networks giving higher added value to the material with high biomass content.[10] This study revealed a class of smart materials which is capable of stress relaxation and self-healing without the addition of any extrinsic catalyst. The use polycarboxylic acid i.e., citric acid, produced in large scale from citrus fruits, blessed the material as self-healable and recyclable. The –COOH groups take part in thermally activated transesterification reaction with β-hydroxyester links generated by the epoxy–acid reaction at elevated temperature without the addition of any extrinsic catalyst.

However, still there is need for the improvement of performance characteristics of these materials for their practical uses. In this regard multiwall carbon nanotubes (MWCNTs) can play an important role in the improvement of performance characteristics of these polymeric materials. Due to the excellent electronic properties, thermal conductivity, and mechanical strength of MWCNTs attracted a great deal of interest as advanced materials and created a high level of activity in materials research for its potential application in various industries.[13,14] MWCNTs also possess outstanding properties, like high aspect ratio, excellent chemical and environmental stability, which makes them ideal candidates as nano reinforcing filler for the polymer based nanocomposites. Inspired from these features of MWCNTs, a number of efforts have been devoted to fabricate MWCNT/polymer nanocomposites in the development of high-performance composite materials.[15-17] The properties of the polymer composites, including tensile strength,[18] tensile modulus,[19] ductility and toughness,[20] glass transition

temperature,[21] thermal conductivity,[22] electrical conductivity,[23] solvent resistance,[24] etc improved significantly due to the incorporation of MWCNTs. However, due to the high cost and limited availability of the MWCNTs, only a few practical applications in industrial fields (electronic and electric appliances) have been recognized till date. The nanocomposites with very low loading of MWCNTs and polymer materials which are derived from sustainable resources can compensate the cost effectiveness of MWCNTs. It is obvious that the improved performances of the nanocomposites will have a role.

It is worth knowing that for the effective nano reinforcement of MWCNTs, homogeneous dispersion of MWCNTs within the polymer matrix and good interfacial adhesion between MWCNTs and polymer matrix is obligatory. In general, MWCNTs agglomerate due to van der Waals attraction and become extremely difficult to disperse and align within polymer matrix. These affect the efficient load transfer from the polymer matrix and the reinforcement of MWCNTs in the nanocomposites. The functionalization of MWCNTs can be regarded as an effective way to achieve better dispersion and strong interfacial interactions, which lead to improve the load transfer across the MWCNTs-polymer matrix interface. Thus, the functionalization of MWCNTs imparts compatibility with the polymer matrix and thereby improves the overall properties of the polymer/MWCNTs nanocomposites.[17] There are several ways for functionalization of MWCNTs including defect functionalization, covalent functionalization, and non-covalent functionalization.[25]

Inspired from these studies, we have used carboxylic acid functionalized multiwall carbon nanotubes (c-MWCNTs) to improve the overall performances of ESO-CA polymer networks. Thus, in this work we have prepared a series of ESO/CA/c-MWCNTs bionanocomposites with different wt % of c-MWCNTs in aqueous solution via sonication treatment. The performances, like thermal stability, tensile strength, elongation at break, scratch hardness, and gloss of the ESO/CA/c-MWCNTs bionanocomposites were investigated as a function of c-MWCNTs content. The in vitro biodegradation of the bionanocomposite films were studied.

6.2 Experimental

6.2.1 Materials

Refined soybean oil was purchased from Adani Wilmer Limited, India. Citric acid monohydrate ($C_6H_8O_7.H_2O$; ≥ 99.5 %; molecular weight = 210 g/mol), hydrogen peroxide (50%), formic acid (85%), and nitric acid were purchased from Merck, India. MWCNTs (purity >97%, diameter = 10–15 nm, length = 0.1–10 µm, density = 1.7–2.1 g/cm^3) were purchased from Redex Technologies Pvt. Ltd., Ghaziabad, UP, India. All the materials were used as received without any further purification.

6.2.2 Preparation of epoxidized soybean oil (ESO)

Epoxidation of soybean oil was carried out in the presence of mixture of formic acid and hydrogen peroxide (Scheme 6.1). The molar ratio of formic acid : double bond : hydrogen peroxide was taken as 0.5 : 1.0 : 1.5. Briefly, 23.74 g (0.5 mol) of formic acid was added to 100 g (1.0 mol double bond) of soybean oil (SO) in a three necked round

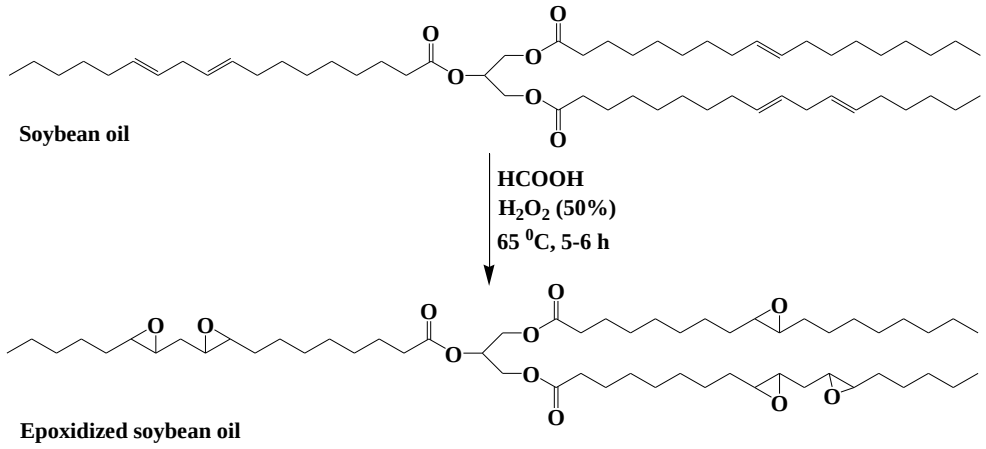

Scheme 6.1: Schematic for the preparation of epoxidized soybean oil.

bottom flask and the reaction temperature was raised to 65 ºC with continuous stirring. Then 105.28 g (1.5 mol) hydrogen peroxide (50%, w/v) was added dropwise (1 mL per 3 min) to the reaction mixture and the reaction continued for 5 h. Since the epoxidation process is exothermic, proper precaution was taken to avoid overheating the reaction

mixture. The resulting mixture was cooled to room temperature and washed with distilled water followed by sodium bicarbonate solution repeatedly until neutral pH was attained. The oily phase was collected and dried over anhydrous sodium sulfate (yield: 91%). The properties like acid value, iodine value, epoxy equivalent weight, viscosity, and average functionality of the prepared ESO are summarized in Table 6.1.

Table 6.1: Physicochemical properties of the ESO.

sample	acid value (mg of KOH/g)	hydroxyl value (mg of KOH/g)	iodine value (g I_2/100g)	epoxy equivalent weight (g/eq)	viscosity at 25 ºC (Pa.s)	average functionality
SO	2.36	3.64	130	---	0.573	---
ESO	3.25	31.50	27	385 ± 2	0.637	3.18

6.2.3 Functionalization of MWCNTs

The carboxylic acid functionalized MWCNTs (c-MWCNTs) were prepared according to the method described previously.[26,27] The pristine MWCNTs (0.5 g) were suspended in concentrated HNO_3 and ultrasonicated for 2 h. The suspension was refluxed with vigorous stirring at 90 °C for 24 h. After cooling at room temperature, the reaction mixture was diluted with 500 mL of deionized water and then filtered through a 2 µm porous filter paper. The filtrated solid was then washed thoroughly with deionized water until the pH became neutral. The collected solid was dried in vacuum oven at 60 °C for 12 h and used for further study.

The c-MWCNTs were quantitatively analyzed by back titration to determine the -COOH concentrations on the surface of c-MWCNTs.[26,28] In a typical method, c-MWCNTs (100 mg) were added into a 15 mL 0.1 N NaOH solution and stirred for 48 h at 30 °C to allow the solid c-MWCNTs to equilibrate with the NaOH solution. The mixture was then filtered and the filtrate was titrated with 0.1 N HCl solution to determine the excess NaOH and the concentration of -COOH groups on c-MWCNTs.

6.2.4 Preparation of ESO-CA networks and their bionanocomposites with c-MWCNTs

The ESO/CA/c-MWCNTs bionanocomposites were synthesized by in situ ring opening polymerization of ESO by an aqueous citric acid solution. In a typical synthesis, citric acid was dissolved in water and ultrasonicated for 2 h with different quantities of c-MWCNTs (1, 2, and 3 wt %) to obtain dispersed suspensions of c-MWCNTs. Then the ESO was added to the c-MWCNTs suspensions with constant stirring at 90 ^{o}C for a period of 0.5 - 0.75 h followed by ultrasonication for 1 h. The resulting mixture was placed overnight in a vacuum oven at 45 °C to remove the moisture and trapped air. After that the mixture was poured on a Teflon sheet by an applicator maintaining the thickness of 0.5 mm and allowed to cure at 120 °C in an oven. The compositions of the bionanocomposites with different wt % of c-MWCNTs are summarized in Table 6.2. It should be noted that in all the formulations stoichiometric ratio of carboxylic acid equivalents and epoxy equivalents was taken as 1:1.

Table 6.2: Compositions of the bionanocomposites.

entry	*sample particulars	ESO (g)	citric acid (g)	water (g)	c-MWCNTs (wt %)
1	CNTC0	3	0.545	0.182	0
2	CNTC1	3	0.545	0.182	1
3	CNTC2	3	0.545	0.182	2
4	CNTC3	3	0.545	0.182	3

*the number denotes the wt % of c-MWCNTs with respect to ESO.

6.3 Instrumentation and methods

6.3.1 Fourier transform infrared spectrometer (FT-IR)

To gain insights into the structural information of prepared bionanocomposites, Fourier transform infrared (FT-IR) spectra of the specimens were recorded on a Nicolet,

Impact 410 FT-IR spectrometer at room temperature over a frequency range of 4000–500 cm^{-1} in KBr medium.

6.3.2 Powder X-ray diffractometer (XRD)

The crystalline structure of the bionanocomposites was studied by using a X-ray diffractometer (Miniflex, Rigaku Japan) with Cu Kα radiation (λ = 0.154 nm) at 30 kV and scanning rate of 0.005° s^{-1} in a 2θ range of 10° to 70°.

6.3.3 Thermogravimetric analysis

To study the thermal stability of the bionanocomposites, thermogravimetric analysis (TGA) was carried out on a Shimazdu TGA 50, thermal analyzer in nitrogen atmosphere at a heating rate of 10 °C min^{-1} in the temperature range 25 °C to 600 °C.

6.3.4 Transmission electron microscopy (TEM)

The distribution and particle size of the c-MWCNTs were studied by transmission electron microscope (TEM, JEOL JEM 2100) at an acceleration voltage of 200 kV.

6.3.5 Mechanical property

The tensile strength, elongation, and elastic modulus of the cured films were analyzed by a universal tensile testing machine (Zwick Z010, Germany) at ambient temperature. The extension rate was 5 mm/min and the load cell was 10-kN, with a gauge length of 40 mm. specimen dimension was 60 mm in length, 10 mm in width, and 0.6 mm in thickness. Scratch hardness test on the cured films was carried out by a scratch hardness tester (Sheen instrument Ltd., UK).

6.3.6 Chemical resistance

The chemical resistance test for the bionanocomposite films was performed to study the effect of chemicals like water, ethanol (25%, aq.), NaOH (2%, aq.), and HCl (10%, aq.). Small pieces of the bionanocomposite films were kept in 100 mL amber glass bottles

containing the aforesaid medium at 30 °C. The percent weight loss of the samples was measured after three weeks of the test by following equation:

$$\% \text{ weight loss} = \left(\frac{W_o - W_t}{W_o} \right) \times 100 \qquad \text{(Eqn. 6.1)}$$

where, W_o and W_t are weight of the specimen at time, t = 0 and t = 21 days of the test respectively.

6.3.7 Evaluation of physical properties

The physical properties like acid value, iodine value, hydroxyl value, and epoxy equivalent weight of the ESO were determined by the methods referred in Chapter 2 and Chapter 3.

6.4 Results and discussion

ESO was prepared from soybean oil with a mixture of formic acid and hydrogen peroxide at 65 ºC. An increase in acid value and hydroxyl value was observed on epoxidation of soybean oil (Table 6.1). The increase in acid value and hydroxyl value may be due the hydrolysis of triglyceride ester and epoxy group respectively in presence of formic acid. The product was low-viscosity, and the structure was confirmed by FT-IR. The ESO/CA/c-MWCNTs bionanocomposites were prepared by mixing the designed components and cured at 120 °C.

6.4.1 Plausible mechanism of formation of the bionanocomposites

Scheme 6.2 presents the plausible mechanism accounting for the epoxy ring opening reaction of ESO by –COOH groups in aqueous solution.[5] The protons produced by the dissociation of -COOH groups in the aqueous solution (Step 1) catalyses the ring opening polymerization reaction. The next step of the reaction is the protonation of the epoxy group (Step 2) followed by attack of the carboxylate anion (Step 3). Although the reaction of epoxy group with carboxylate anion leading to a β-hydroxyester is favored, the hydrolysis of epoxy groups also takes place (Step 4). Considering the water used to

dissolve citric acid and the water added with citric acid, the initial molar ratio H_2O/COOH is approximately 1.6 and less reactive central -COOH group of citric acid can reinforce the hydrolysis reaction (Step 4). Hence some of the -COOH groups remain unreacted and thus can take part in thermally activated transesterification reactions during postcure at 160 ºC with the -OH groups produced by Step 3 & 4.[10] The plausible cross-linked structure of the ESO/CA/c-MWCNTs bionanocomposites is presented in Scheme 6.3. The bionanocomposites were postcured at 160 °C for 10 h and the effects on thermal and mechanical properties were investigated.

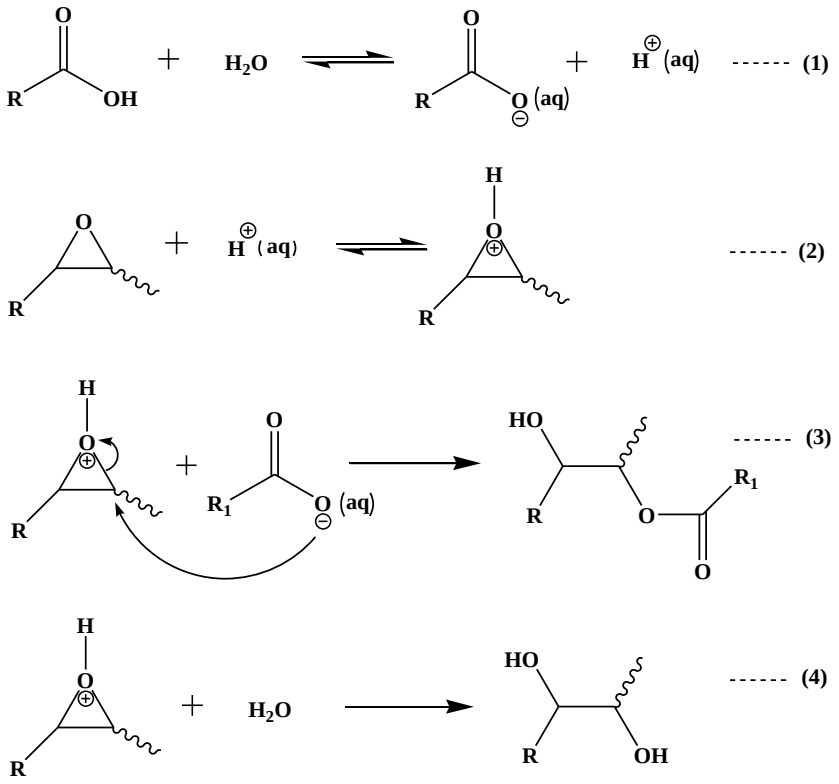

Scheme 6.2: Plausible reaction mechanism accounting for the epoxide ring opening by an aqueous citric acid solution.

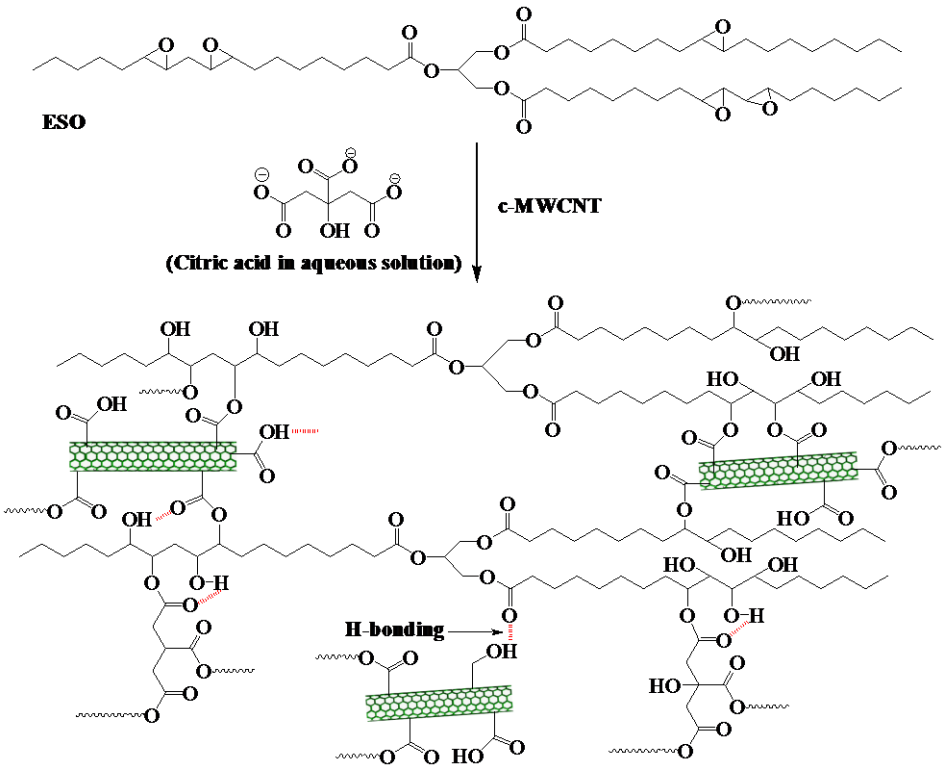

Scheme 6.3: Plausible Cross-linked structure of the ESO/CA/c-MWCNTs bionanocomposite.

6.4.2 Spectroscopic analysis of the bionanocomposites

The FT-IR spectra of MWCNTs, c-MWCNTs, ESO, ESO-CA networks (CNTC0), and the bionanocomposite are presented in Fig. 6.1. The peak at around 1632 cm^{-1} is attributed to the IR active phonon mode of the MWCNTs (Fig. 6.1a) and the peaks at around 1730, 1071, and 1163 cm^{-1} apparently correspond to the stretching vibrations of the carboxylic acid groups (Fig. 6.1b). The broad peak at 3415 cm^{-1} is assigned to the -OH stretching of the terminal carboxyl group.[29] The results indicate that the carboxylic acid groups were successfully introduced at both ends and on the sidewalls of the MWCNTs by chemical treatment with nitric acid. In the surface treatment process, the free oxygen atoms released by nitric acid react with unstable carbon atoms to generate -COOH groups on the surface of the MWCNTs.[15] In the FT-IR spectra of ESO (Fig. 6.1c) the peak at 829 cm^{-1} attributed to epoxy group was observed to be disappeared on in the ESO-CA networks (Fig. 6.1d) and the bionanocomposites (Fig. 6.1e). It implies that the epoxy groups have been consumed in the ring opening polymerization reaction with citric acid in

aqueous solution.[5,10] The broadening of the peak at 3450 cm^{-1} can be assigned to hydroxyl groups generated in the ring opening polymerization reaction (Scheme 6.2). Moreover, the shifting of the C=O stretching frequency on polymerization indicates some sort of structural modifications around the carbonyl groups. It may be due to the H-bonding interaction of C=O group with c-MWCNTs and the -OH groups generated during the ring opening polymerization reaction.

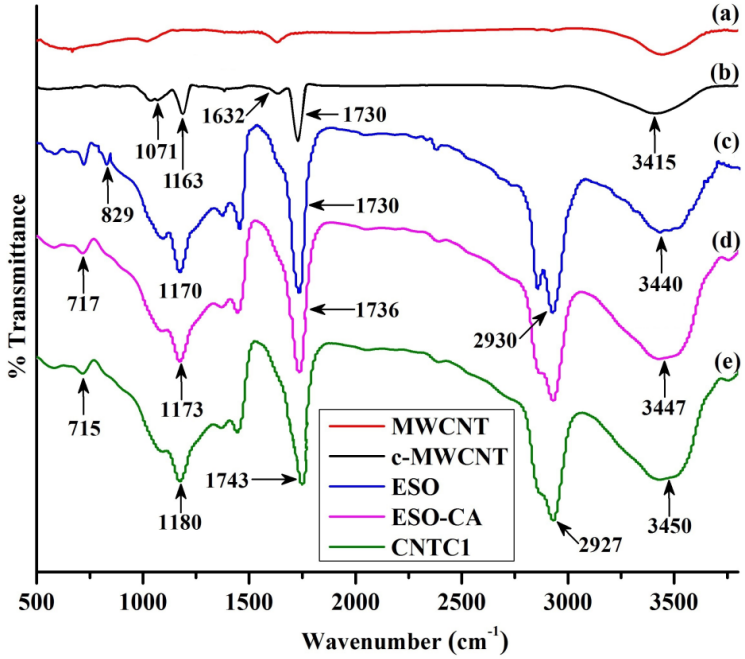

Fig. 6.1: FT-IR spectra of (a) MWCNTs, (b) c-MWCNTs, (c) ESO-CA networks, and (d) bionanocomposites (CNTC1).

6.4.3 XRD analysis

Fig. 6.2 presents the X-ray diffraction data for the neat c-MWCNTs and the ESO/CA/c-MWCNTs bionanocomposites with different wt % of c-MWCNTs. The neat polymer exhibits a broad scattering at 2θ values between 35 to 55°. This indicates the amorphous nature of the ESO-CA polymer networks. For the neat c-MWCNTs, a signal at 25.55° corresponding to (002) plane having interlayer distance of 0.357 nm, while the signal belonging to (100) plane appears at around 43.20°. These two peaks reveal the graphite like structure and presence of small amounts of catalytic particles inside the walls

of c-MWCNTs, respectively.[29,30] The broadening of the peak at 25.55° strongly suggests the partial oxidation of few of the outer layers of c-MWCNTs in presence of concentrated nitric acid. Moreover, on oxidation an increase in interlayer distance of c-MWCNTs is observed as compared to the neat MWCNTs (0.334 nm). It is due to the fact that in the presence of strong acids the most unstable carbon atoms get oxidized and converted into –COOH groups, which are intervening between the layers of c-MWCNTs.

The occurrence of the peaks at 2θ 25.55° and 43.20° in the X-ray diffraction of the bionanocomposites indicate the successful incorporation of c-MWCNTs in the ESO-CA polymer networks. The formation of the ESO/CA/c-MWCNTs bionanocomposites was facilitated by the strong H-bonding and covalent interactions of the c-MWCNTs with the ESO-CA polymer networks. It is noticeable that the intensity of the peaks increases gradually with c-MWCNTs content. It is a result of the higher crystallites of c-MWCNTs in the bionanocomposites with increasing c-MWCNTs content.[31]

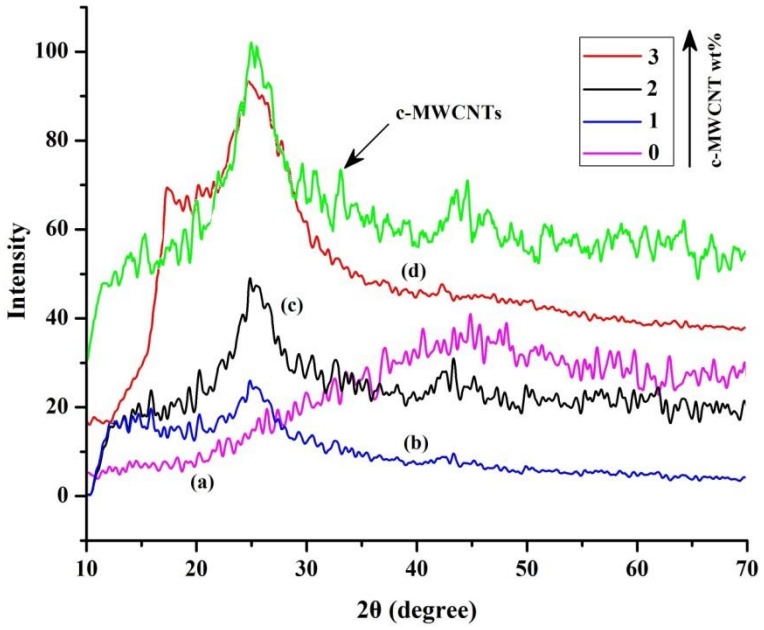

Fig. 6.2: X-ray diffraction of (a) CNTC0, (b) CNTC1, (c) CNTC2, and (d) CNTC3.

6.4.4 Morphology of the bionanocomposites

The microstructure of c-MWCNTs and ESO/CA/c-MWCNTs bionanocomposites has been visualized by using HR-TEM and the micrographs are presented in Fig. 6.3. As evident from the HRTEM study, the stable and uniform dispersion of the c-MWCNTs within the ESO-CA networks is instrumental in comprehending the improvement of the performance characteristics of the bionanocomposites. The strong dipolar and H-bonding interactions between –COOH groups of c-MWCNTs and -OH, -COOH, -COOR, and epoxy groups of ESO-CA networks facilitate stable and uniform dispersion of c-MWCNTs in the bionanocomposites. As compared to the neat c-MWCNTs, having an average outside diameter of 20-25 nm, the c-MWCNTs in the bionanocomposites showed a high average outer diameter of 35-40 nm. The increase in diameter of c-MWCNTs in the ESO/CA/c-MWCNTs bionanocomposites indicates the presence of ESO-CA polymer layers anchoring on the surface of the c-MWCNTs.

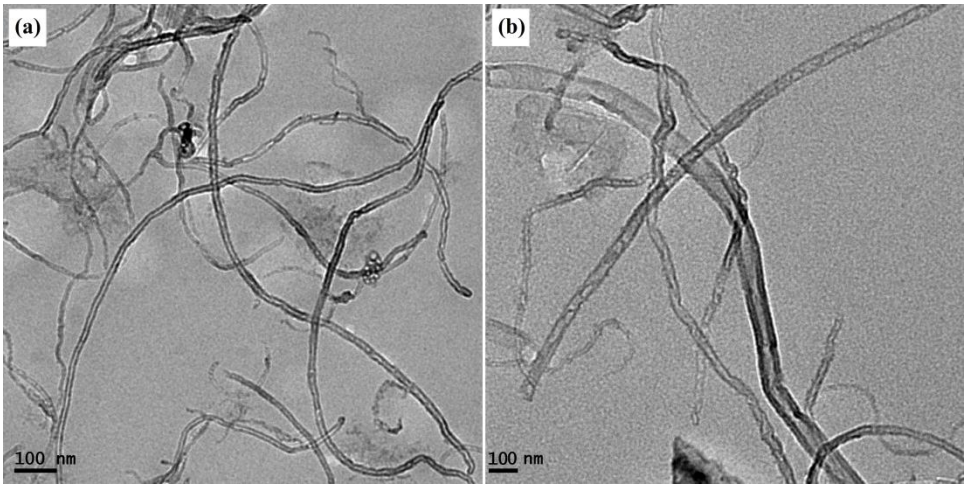

Fig. 6.3: TEM micrographs of (a) c-MWCNTs, and (b) bionanocomposites (CNTC1).

6.4.5 Curing study and mechanical properties

The curing time of the bionanocomposites was recorded and summarized in Table 6.3. It was observed that the curing time of the bionanocomposites decreases significantly with c-MWCNTs content. The curing time was reduced to 6.5 h with 3 wt % c-MWCNTs loading in the bionanocomposites, whereas the same for the neat ESO-CA networks was 10 h. It can be well explained by using Arrhenius theory, which refers to that the reaction

rate constant is dependent on reaction temperature, collision factors as well as the activation energy. In relation to this study, it is understood that the incorporated of c-MWCNTs into the polymer networks restrict the diffusion of the reactive species for cross-linking due to filler-filler and/or filler-polymer interaction through covalent and/or electrostatic interactions. This implies that the c-MWCNTs caused an increase in the collision factor of the reactive species around the vicinity in the cross-linking system. Therefore, this resulted in an auto-acceleration reaction of the ESO/CA/c-MWCNTs bionanocomposite system.[32,33] Moreover, the incorporation of c-MWCNTs increases the activation energy of the reactive species and thereby hastens the rate of cross-linking reaction. It is obvious that the better dispersion and strong interactions between c-MWCNTs and ESO-CA polymer networks resulted in increase in activation energy of the ESO/CA/c-MWCNTs bionanocomposites.

The properties such as scratch hardness, tensile strength, elongation at break, toughness, and gloss of the bionanocomposites are listed in Table 6.3. Significant improvement in mechanical properties of the ESO-CA based bionanocomposite was observed by the incorporation of c-MWCNTs. It can be attributed to the strong interfacial adhesion between the ESO-CA polymer networks and the c-MWCNTs. The covalent bonding between the epoxide groups of ESO and –COOH groups on the surface of the c-MWCNTs and H-bonding interactions among the polar functionalities facilitated the strong interfacial adhesion (Scheme 6.3). The increment in scratch hardness of the bionanocomposites with the c-MWCNTs content is due to the enhanced strength of the nano reinforcing c-MWCNTs and flexibility of the long hydrocarbon chains the ESO. The ESO-CA polymer networks exhibited a tensile strength of 0.68 MPa which is increased to 2.72 MPa with the incorporation of 3 wt % c-MWCNTs. The four fold increment in tensile strength of the ESO/CA/c-MWCNTs (3 wt %) bionanocomposites as compared to the ESO-CA polymer networks strongly suggests the strong interfacial adhesion between the ESO-CA polymer networks and the c-MWCNTs. Moreover, these interactions facilitated the homogeneous dispersion of the c-MWCNTs within the ESO-CA polymer networks and led to the formation of dense cross-linked structure, which hinder the mobility of the polymer chains and resulted the improve mechanical properties of the

bionanocomposites.[34] In other words, the nano-reinforcing effect imparted by the c-MWCNTs is responsible for providing the mechanical integrity to the ESO/CA/c-MWCNTs bionanocomposites. The decrease in the elongation at break of the bionanocomposites is justified by the reduced mobility of the polymer chains due to the incorporation of c-MWCNTs. The obtained toughness of the ESO/CA/c-MWCNTs bionanocomposites is a result of the combined effect of nano reinforcement of c-MWCNTs and as well as the flexibility of the long fatty acid chains.[20] The increment in the gloss with c-MWCNTs content in the bionanocomposites indicated that the cured films possess good dimensional stability and smooth surface morphology.

Table 6.3: Performance characteristics of the bionanocomposites.

properties	c-MWCNTs (wt %)			
	0	1	2	3
curing time (h)	10.0	9.0	8.0	6.5
scratch hardness (kg)*	1.6	2.3	2.9	3.6
tensile strength (MPa)	0.63	1.47	2.14	2.72
elongation at break (%)	58	45	35	23
toughness	29	37	51	60
gloss	72	73	75	78

* Limit of the instrument for scratch hardness was 10.0 kg (maximum). #Limit of the instrument for impact strength was 100 cm (maximum).

6.4.6 Thermogravimetric analysis

The thermal stability and degradation pattern of the ESO/CA/c-MWCNTs bionanocomposites were assessed by thermogravimetry under nitrogen atmosphere. Fig. 6.4 present TGA weight loss and weight loss derivative curves of the ESO/CA/c-MWCNTs bionanocomposites with different wt % of c-MWCNTs. The TGA data such as initial degradation temperature (T_i), decomposition temperature at different at weight losses (T_d), maximum pyrolysis temperature (T_m), and residual weight (%) are summarized in Table 6.4. Significant improvement in thermal stability of the bionanocomposites is observed by the incorporation of c-MWCNTs; for example, the T_i

for the pristine ESO-CA networks is 289 °C, whereas the same for the ESO/CA/c-MWCNTs bionanocomposite with 3 wt % c-MWCNTs is increased by 38 °C. The increase in thermal stability of the bionanocomposites with increasing c-MWCNTs content is attributed to the nano-mechanical interlocking of the c-MWCNTs within the ESO-CA polymer networks via strong adherence of functionalities onto the nanotube

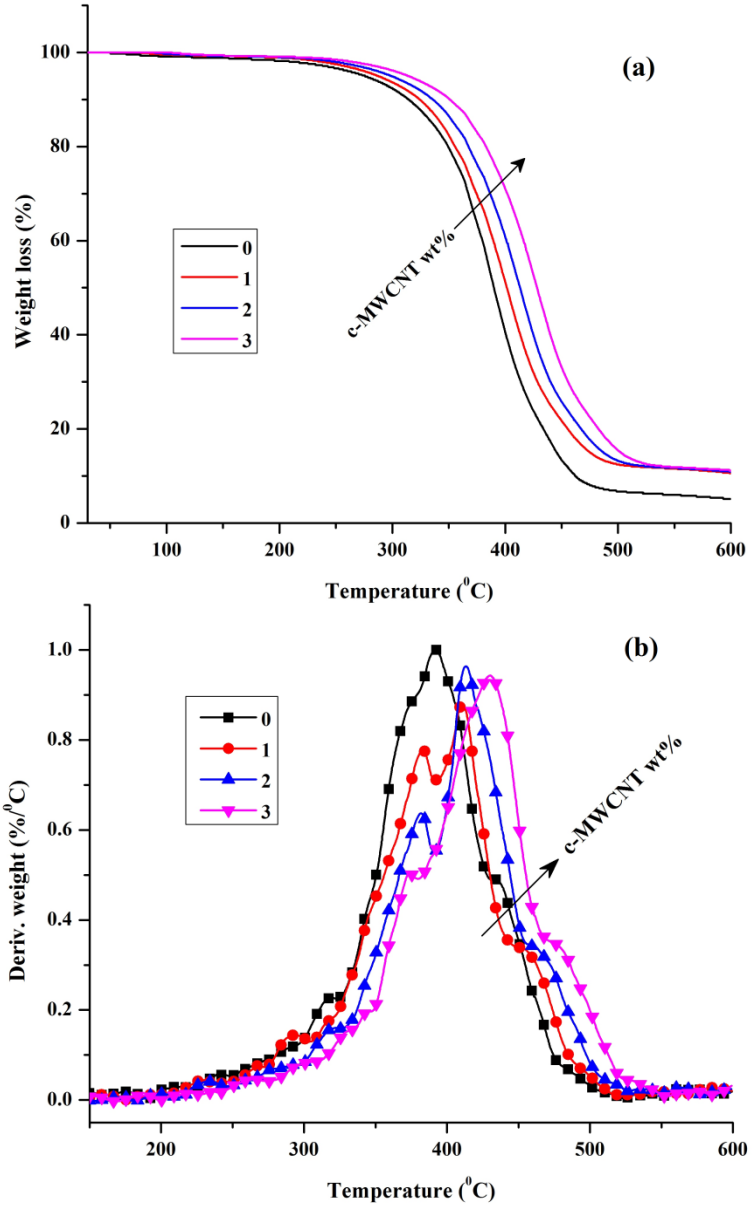

Fig. 6.4: TGA (a), and DTG (b) curves for the bionanocomposites with different wt% of c-MWCNTs.

surface (Scheme 6.3). It is well defined that the degradation of polymer occurs with the free radical formation at the weak bonds followed by radical transfer to adjacent chains through inter chain reaction. Due to the strong interfacial interaction between c-MWCNTs and ESO-CA networks the polymer chain mobility is reduced and the chain transfer reaction is suppressed and thereby delays the degradation process.[35] The covalent bonding between the epoxide groups of ESO and –COOH groups on the surface of the c-MWCNTs resulted in a strong interfacial adhesion between the polymer matrix and the c-MWCNTs. The increment in weight residue of the bionanocomposites at 600 °C (Table 6.4) reflects the presence of thermo-stable c-MWCNTs.

Table 6.4: Thermal degradation data of the bionanocomposites.

c-MWCNTs wt %	T_i (°C)	decomposition temperature (T_d, °C) at different wt losses				T_m (°C)	residual wt (%)
		$T_{5\%}$	$T_{15\%}$	$T_{30\%}$	$T_{50\%}$		
0	289	275	335	367	390	392	5.12
1	300	287	342	375	402	406	10.57
2	311	298	354	386	413	413	10.72
3	327	312	370	402	428	431	10.91

T_i = Initial degradation temperature; T_m = maximum pyrolysis temperature.

6.4.7 Chemical resistance

The chemical resistance test for the bionanocomposites was performed in water, NaOH (1%, aq.), HCl (10%, aq.), and ethanol (20%, aq.) and the results are given in Table 6.5. The ESO/CA/c-MWCNTs bionanocomposite films exhibited excellent resistance to the aforesaid chemical environment. It can be attributed to the highly cross-linked and rigid structure of the bionanocomposites. In addition, the effect became more pronounced with increasing c-MWCNTs content in the bionanocomposites. It is due to the fact that with increasing the concentration of c-MWCNTs, the compactness and rigidity of the structure increases and prevents the solvent penetration. But due to the presence of

hydrolysable ester linkages in the polymer networks, the alkali resistance of the bionanocomposites is relatively poor.

Table 6.5: Chemical resistance (% wt loss) test for the bionanocomposite films.

entry	c-MWCNTs (wt %)	chemical environment			
		water	ethanol (25%, aq.)	NaOH (2%, aq.)	HCl (10%, aq.)
1	0	0	0	2.63	2.84
2	1	0	0	1.65	1.92
3	2	0	0	0.96	1.53
4	3	0	0	0.48	1.21

6.4.8 Effect of postcuring on thermal and mechanical properties of the bionanocomposites

The influence of postcuring of the bionanocomposite films at 160 ºC was investigated by means of thermal and mechanical properties. TGA curves of the postcured bionanocomposite films are presented in Fig. 6.5 and the overall performances are summarized in Table 6.6. It was observed that in all the cases the thermal stability and tensile strength of the bionanocomposite films improved significantly with decreased elongation at break. The improvement in thermal and mechanical properties of the bionanocomposite films on postcuring at 160 ºC can be attributed to the increased cross-linking density of the polymer networks. The molecular rearrangements produced by thermally activated transesterification reactions of -OH groups generated during the ring opening polymerization reaction (Scheme 6.3, Step 3 & 4) with residual -COOH groups result the increased cross-linking density of the polymer networks.[10] Most of the citric acid units had taken part in cross-linking reactions and hence producing the observed increase of the thermal and mechanical properties of the bionanocomposites. It was observed that the improvement in thermal and mechanical properties of the bionanocomposites became more pronounced with increase in c-MWCNTs content, for

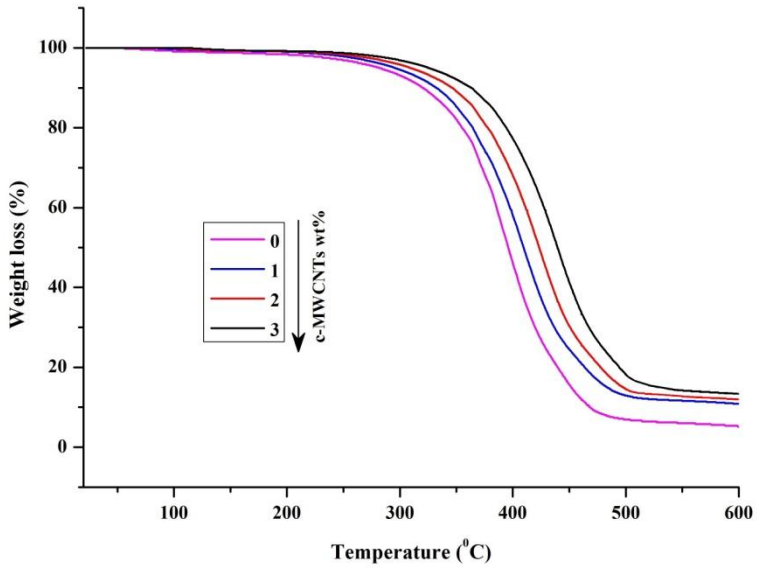

Fig. 6.5: TGA curves for the postcured bionanocomposite films.

Table 6.6: Performance of the postcured bionanocomposite films.

sample	curing conditions	tensile strength (MPa)	elongation at break (%)	scratch hardness (kg)	T_i (ºC)
CNTC0	120 ºC	0.63	58	1.5	289
	*160 ºC	0.86	42	1.7	297
CNTC1	120 ºC	1.47	45	2.1	300
	*160 ºC	1.78	33	2.4	312
CNTC2	120 ºC	2.14	35	2.6	311
	*160 ºC	2.49	21	2.9	326
CNTC3	120 ºC	2.72	23	3.1	327
	*160 ºC	3.14	15	3.5	343

*postcured at 160 ºC for 10 h.

instance the T_i for ESO-CA was increased by 8 °C, whereas the same for the bionanocomposite with 3 wt % c-MWCNTs, was increased by 16 °C. Similarly, the tensile strength for the bionanocomposite with 3 wt % c-MWCNTs, was enhanced by 0.42 MPa as compared to the neat ESO-CA networks (0.23 MPa). It was attributed to the fact that the -COOH groups on the surface of the nanotubes had taken part in the

transesterification reaction with the –OH groups of the ESO-CA polymer networks, and hence led to the formation of dense cross-linked structure of the bionanocomposites. The reduced mobility of the polymer chains due to the incorporation of c-MWCNTs justified the decrease in elongation at break of the bionanocomposites.

6.5 Conclusion

- The study revealed a class of *green* bionanocomposites which was prepared by an *in situ* solvent free and catalyst free method.
- Citric acid, which is produced at large scale from citrus fruits, is an effective curing agent for the epoxy resins.
- The bionanocomposites with high bio-based content exhibited impressive performance characteristics.
- The bionanocomposites are thermally stable upto 327 °C and can be improved further upto 343 °C by postcuring at 160 °C for 10h.
- The nanocomposite films exhibited tensile strength of 2.18 MPa with 35% elongation at break.
- The strong H-bonding and covalent interactions of the c-MWCNTs with the ESO-CA polymer networks resulted in improved performance characteristics of the bionanocomposites.
- The molecular rearrangement produced by thermally activated transesterification reaction of -OH groups with residual -COOH groups on postcuring stage resulted increase in cross-linking density of the polymer networks. However, the effect was more pronounced with the high concentration of c-MWCNTs in the bionanocomposites.
- The overall results of the study suggest the bionanocomposites as sustainable material for industrial applications.

References

1. Meier, M.A.R., et al. *Chem. Soc. Rev.* **36** (11), 1788-1802, 2007.
2. Lligadas, G., et al. *Biomacromolecules* **11** (11), 2825–2835, 2010.
3. Espinosa, L.M., & Meier, M.A.R. *Eur. Polym. J.* **47** (5), 837–852, 2011.
4. Biermann, U., et al. *Int. Ed.* **50** (17), 3854–3871, 2011.
5. Gogoi, P., et al. *ACS Sustainable Chem. Eng.* **3**(2), 261−268, 2015.
6. Sun, X.S., & Wool, R.P. *Bio-Based Polymers and Composites*, Academic Press, Elsevier, Amsterdam, 2005.
7. Okieimen, F.E., et al. *Ind. Crop. Prod.* **15** (2), 139–144, 2002.
8. Hilker, I., et al. *Chem. Eng. Sci.* **56** (2), 427–432, 2001.
9. Klaas, M.R., & Warwel, S. *Ind. Crop. Prod.* **9** (2), 125–132, 1999.
10. Altuna, F.I., et al. *Green Chem.* **15** (12), 3360-3366, 2013.
11. Zhang, C., et al. *Green Chem.* **15** (6), 1477–1484, 2013.
12. Wang, Z., et al. *Macromolecules* **45** (22), 9010−9019, 2012.
13. Kim, J.Y. *J. Appl. Polym. Sci.* **112** (5), 2589–2600, 2009.
14. Kim, J.Y., et al. *Eur. Polym. J.* **45** (2), 316–324, 2009.
15. Kar, P., & Choudhury, A. *Sens. Actuators, B* **183**, 25– 33, 2013.
16. Kwon, J.Y., & Kim, H.D. *J. Appl. Polym. Sci.* **96** (2), 595–604, 2005.
17. Sahoo, N.G., et al. *Prog. Polym. Sci.* **35** (7), 837–867, 2010.
18. Kanagaraj, S., et al. *Compos. Sci. Technol.* **67** (15), 3071–3077, 2007.
19. Jin, S.H., et al. *Compos. Sci. Technol.* **67** (15), 3434–3441, 2007.
20. Yang, B.X., et al. *Nanotechnology* **18** (12), 125606(1–7), 2007.
21. Pham, J.Q., et al. *J. Polym. Sci., Part B: Polym. Phys.* **41** (24), 3339–3345, 2003.
22. Singh, I.V., et al. *Int. J. Numer. Method. H.* **17** (8), 757–769, 2007.
23. Grossiord, N., et al. *Chem. Mater.* **19** (15), 3787–3792, 2007.
24. Guo, H., et al. *Polymer* **46** (9), 3001–3005, 2005.
25. Hirsch, A. *Angew. Chem. Int. Ed.* **41** (11), 1853–1859, 2002.
26. Atieh, M.A., et al. *Bioinorg. Chem. Appl.* **2010**, 1-9. 2010.
27. Worsley, K.A., et al. *J. Am. Chem. Soc.* **131** (50), 18153-18158, 2009.
28. Davis, R.H., *Int. J. Thermophys*. **7** (3), 609–620, 1986.

29. Wu, T.M., & Lin, Y.W. *Polymer* **47** (10), 3576–3582, 2006.
30. Tamilarasan, P., & Ramaprabhu, S., *J. Mater. Chem. A* **2** (34), 14054–14063, 2014.
31. Abdolmaleki, A., et al. *Prog. Org. Coat*. **80**, 71–76, 2015.
32. Wang, X., et al. *Eur. Polym. J*. **48** (6), 1034-1041, 2012.
33. Sriloy, N., et al. *Macromol. Res.* **18** (4), 372-379, 2010.
34. Yuan, W., & Chan-Park, M.B. *ACS Appl. Mater. Inter.* **4** (4), 2065–2073, 2012.
35. Mbhele, Z.H., et al. *Chem. Mater*. **15** (26), 5019-5024, 2003.